

ARROW Structures Applied to MOEMS: Optical Accelerometer

A. Llobera¹, J. A. Plaza¹, I. Salinas², J. Berganzo³, J. Garcia³, J. Esteve¹ & C. Domínguez¹

1. IMB-CSIC. Campus UAB 08193
Cerdanyola, Barcelona, Spain. Tel. 935947700. Fax. 935801496
andreu.llobera@cnm.es
2. Dept. de Física Aplicada, Universidad de Zaragoza
3. Ikerlan, Departamento de Electrónica y Componentes

Areas de interés. MOI, SEN

Palabras clave: Accelerómetros, MOEMS, Óptica Integrada, Tecnología

1.- Summary.

ARROW (AntiResonant Reflecting Optical Waveguides) structures have been tested for the fabrication of MOEMS (Micro-Opto Electro Mechanical Systems), concretely, the fabrication and characterization of an optical accelerometer based on silicon technology is presented. On the basis of a quad beam accelerometer design, a sensing ARROW structure has been placed on the seismic mass. Its misalignment with the waveguides located at the frame allows measuring the acceleration. The mechanical structure has been designed so as to have a mechanical span of 2 μm , that provides with a sensitivity of 4.6 dB/g. Although high insertion losses have been observed due to imperfections in polishing the V-grooves with glass anodic bonding, the experimental sensitivity has been measured to be 2.3 dB/g.

2.- Introduction.

To overcome the inherent problems of electrical-based accelerometers, for example temperature dependence, low sensitivity and non stable output under electromagnetic interference (EMI) [1], there has been several proposals of optical-based accelerometers, both using integrated optics [2] and fiber optics [3]. The complete immunity against EMI and the possibility of having the light sources far from the device also makes them extremely useful in explosive atmospheres or where a strong electromagnetic field is present.

Up to date, the most common light guiding structures used on optical accelerometers have a high refractive index etched layer (frequently silicon nitride) in a cantilever configuration. Although they could be considered as optimum for MOEMS applications, it has to be noted that these waveguides normally have thicknesses around 0.2 μm . If it is taken into account that a standard monomode optical fiber has a 4 μm core, the high difference between the cross section of both structures is the main responsible of the high insertion losses (>20 dB) of these waveguides in the visible range when light is inserted by end-fire coupling.

In order to overcome the high insertion losses of the high step-index waveguides it is necessary to obtain core dimensions similar to that of the single mode fiber optics. This property can be obtained by ways of the ARROW structures [4], the configuration of which is shown in fig. 1. Guiding is achieved via the Fabry Perot interferometer placed beneath the core. With a fixed core thickness (d_c) and known refractive indexes of the core and the two cladding layers (n_c , n_1 and n_2 , respectively), there exist some values for the first and second cladding layers (d_1 and d_2) where ultra-high reflection (>99.96%) at the core-1st cladding boundary is observed for the TE_0 . Generally, the modes of these structures are leaky modes since all of them present losses. Nevertheless, if the antiresonant pair is properly configured, theoretical losses for the fundamental mode are as low as 0.08dB/cm. On the contrary, higher order modes are filtered out since the antiresonant layers are not properly sintonized for them. Hence, this structure has monomode behavior for core thickness of the same size as the fiber optics, minimizing the insertion losses.

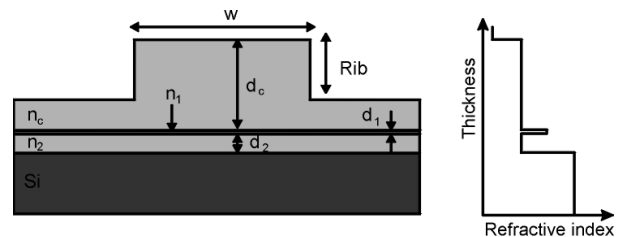


Fig. 1: Standard configuration and refractive index profile of ARROW structures. The darker the grey, the higher the refractive index is.

3. Design and Simulation.

The basic configuration of the accelerometer is presented in fig. 2. The quad beam mechanical structure has a flat displacement in the sensing direction (y-axis). Thence, the misalignment between the waveguides located at the frame and at the mass is only produced in one axis. In order to collect as much light power as possible, the beam broadening in each cut has been compensated by making the waveguides progressively wider in the x-axis (14 μm , 30 μm and 50 μm the input, the sensing and the output waveguide, respectively). Nevertheless, the most important broadening is produced in the y-axis, and it has been considered by reducing the step distance to 24 μm . If the mass was broken, the configuration will be an input and output aligned waveguides distanced a length slightly larger than the seismic mass (4000 μm). Thence, extremely high losses should be obtained, conferring the accelerometer with an auto-test system. Finally, the proposed accelerometer is a combination of two complementary technologies: the 3d micromechanization of the silicon, which requires single layers in order not to have bending due to differences in the thermal expansion coefficients, and the ARROW structure technology, which is a multilayer structure with high mechanical stresses. The combination of both technologies can be achieved if the waveguides are only placed in the bulk parts of the accelerometer (i.e. in the middle of the seismic mass) and maintaining the most sensitive silicon parts of the accelerometer (the beams and the corners) free of any other material than silicon.

Optical simulations of the device losses as a function of the seismic mass displacement were done using the Finite Difference Method (FDM) together with the Beam Propagation Method (BPM). Although $\text{Si}_3\text{N}_4/\text{SiO}_2$ -based ARROW structures had previously been studied [5], it was necessary to analyze the effects of the misalignment between the waveguide on the seismic mass and the waveguides located at the frame

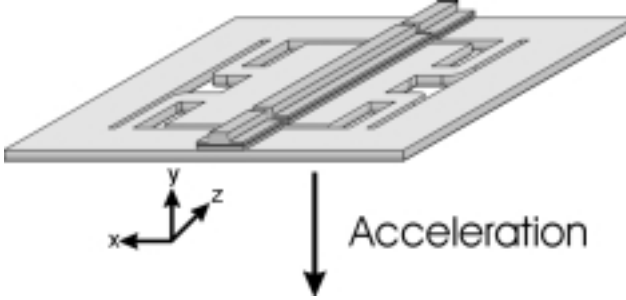


Fig. 2: Scheme of the quad beam optical accelero-meter design.

By ways of these simulation methods, it was possible to define two linear regions, with an optical sensitivity of 4.6 dB/g into which the losses are proportional to the misalignment. In order to confirm the behavior predicted by simulations, the span of the accelerometer was fixed to 2 μm . Once the working region was established, the mechanical optimization of the structure was done via the Finite Element Method (FEM) using ANSYS 5.7. The beams of the accelerometer were designed to have a mechanical sensitivity of 1 $\mu\text{m}/\text{g}$. Thence, the analytical total losses at maximum displacement (1 μm) were 4.6 dB. The cross-sensitivities were also simulated and are presented in table 1. It can be observed that although misalignment obtained matched with the expected mass movement, there exists significant cross acceleration effects: The mass displacement is 0.202 $\mu\text{m}/\text{g}$ for z-accelerations and 0.105 $\mu\text{m}/\text{g}$ for x-accelerations. It has to be noted, however, that since the waveguide is located at the center of the seismic mass, movements on the x direction would not affect its relative position. Thus, the device is completely insensitive to accelerations in the x direction. Modal simulations were done to estimate the natural frequency of the devices. The simulated frequency for the lowest mode is 489 Hz.

Accel [1.0 g]	Maximum mass displac. (μm)	Waveguides misalignment (μm)	Optical losses (dB/g)
Y-axis	1.050	1.050	4.6
X-axis	0.105	0.000	0
Z-axis	0.202	0.202	0.8

Table 1: Maximum displacement of the mass and misalignment between the waveguides on the frame and on the mass versus the three directions of the acceleration.

4.- Fabrication.

4.a ARROW Waveguide Fabrication

Accelerometers were fabricated on a N type, (100) oriented, 450 μm thick BESOI (Bond and Etch Back Silicon On Insulator) wafers from ShinEtsu. Thickness of the upper silicon and buried silicon layers are 15 μm and 2 μm , respectively. In these substrates is grown the second cladding layer (2 μm of silicon dioxide). First cladding is a 0.38 μm LPCVD silicon nitride. Core layer consists in a PECVD-deposited silicon oxide, with refractive index $n=1.485$. This layer is 3.5 μm etched using RIE in order to assure cross section confinement. Finally, a 2 μm PECVD silicon oxide layer ($n=1.46$) was deposited over the waveguides so as to protect them against dust or scratches that would cause an increase of the device losses, not due to the working principle, but to defects in its guidance properties. The following step was the complete removal of all the deposited layers from the substrate except where the rib has been defined (fig. 3). Concretely, the technological process mask were designed so as to leave the ARROW structure only at 100 μm in distance from the rib.

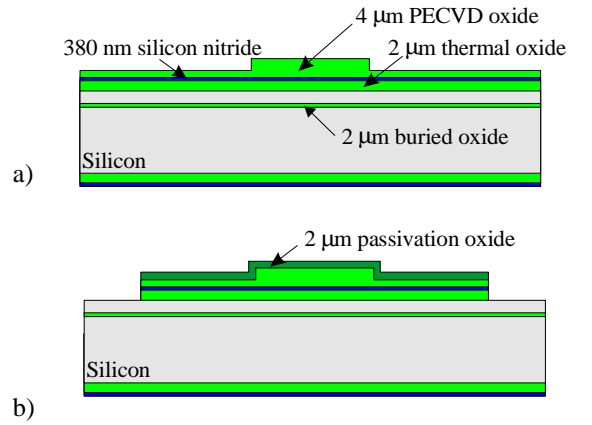


Figure 3: a) ARROW waveguide definition and b) release of the ARROW layer where unnecessary.

4.b Mechanical Structure Fabrication

Layer thicknesses (PECVD silicon oxide, LPCVD silicon nitride and thermal silicon oxide) to be etched were significantly high. This forces to use aluminium as a mask material. Micromechanical structure was defined in two steps: Firstly, an anisotropic etching in KOH at the back side of the wafer provided the three-dimensional structure. Anisotropic etching was done in KOH, with the etching automatically stopped at (111) planes and when the buried silicon oxide layer is reached (fig. 4) a lithographic step with 6 μm thick MAP-245.5 photoresist from Micro AllResist, followed by a dry etching (RIE) at the front side released the accelerometer.

As can be observed in fig. 5a, the shadowing mask effect appeared during the dry etching process, which prevented from releasing the structure. This inappropriate photolithographic step can be understood if it is taken into account that there was a high step (8.38 μm) between the silicon substrate and the passivation layer (that forces using a thick photoresist to cover it). Thence, in order to have a good definition of the seismic

mass on the front side, it was necessary to do an over exposition. As can be observed in fig. 5b, results obtained were clearly satisfactory and seismic mass was liberated from the frame.

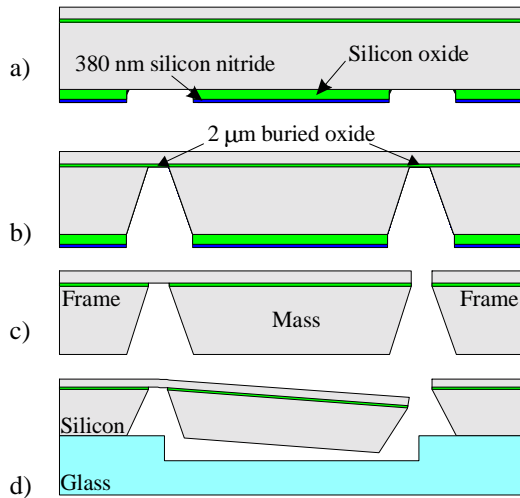


Figure 4: Fabrication process for the mechanical structures.

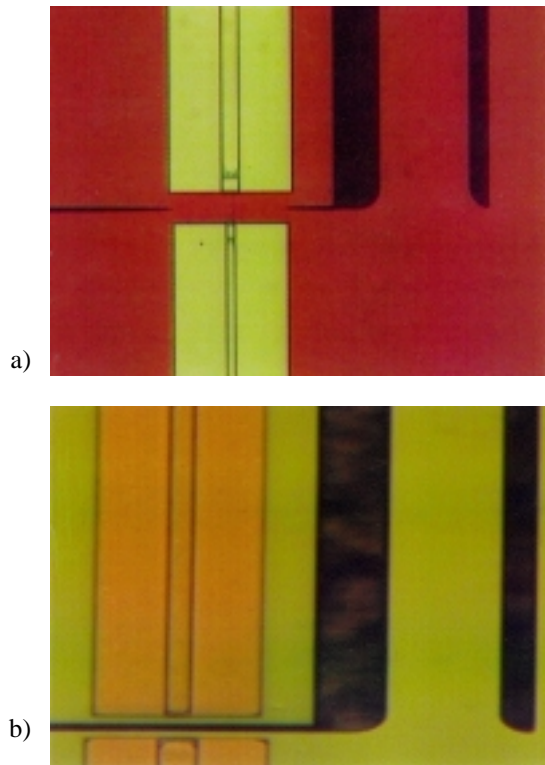


Fig 5: Shadow mask problem during the dry etching a) with standard photolithographic step, b) after overexposure (b).

Although the accelerometer fabrication could be considered as finished at this point, the devices were extremely fragile and cracked easily. In addition, the stresses introduced by the package could negatively affect the performance of the accelerometer. For these reasons the silicon nitride and the silicon oxide were removed from the backside of the wafer and a 1 mm glass wafer (Pyrex #7740) with cavities previously mechanized was bonded on the back side of the silicon wafer, as shown in fig. 4d. The depth of the cavities on the glass defines the

damping of the accelerometer. The presented accelerometers have a theoretical Q factor of 20 for cavities of 80 μm depth. After sawing, the final dimensions of the chips are 6.2mm x 6.2 mm.

5. Characterization

Reference waveguides were measured by end-fire coupling so as to determine the radiation and insertion losses at $\lambda=633$ nm and provided with results of 0.3 dB/cm and 2.5 dB respectively. First measurements done with the optical accelerometer showed losses of 6.8dB. However, both the input and output fiber optics were able to move freely. Then, it was not possible to do an accurate characterization of the device, since it was the uncertainty if the measured losses were due to the seismic mass displacement or, on the contrary, to a misalignment between the input/output fiber optics and the accelerometer. Placing the fiber optics in V-groove made of silicon solved this problem, as shown in fig. 6a. The accelerometer was firstly fixed to a mechanized aluminum piece that has a slight minor length than the accelerometers. V-grooves were then able to move in the three axis until they were correctly aligned, being then glued. When the glue dried, two self-aligned pieces were placed underneath the V-grooves so as to provide the whole structure with robustness, as shown in fig. 6b.

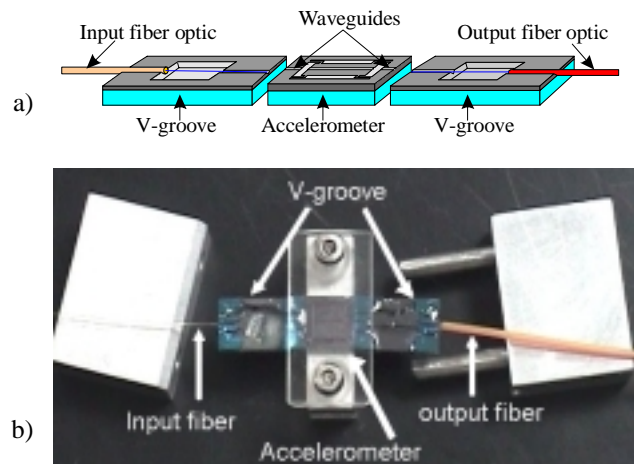


Figure 6: a) Schematic view of the V-grooves-accelerometer system and b) final mounting step, with the fibers on the V-grooves glued to the accelerometer

Light injection by end-fire coupling requires completely flat facets in order to minimize insertion losses. Although it is relatively simple to obtain high-quality facets by silicon polishing, results are not so optimal when a silicon-glass substrate has to be polished. The difference on the stiffness between both materials causes to have a tapered facets and defects on it. This is the main reason why after stacking the accelerometer and the V-grooves, losses increased until 18.3dB, which is 2 times higher than the value obtained by simulations. Nevertheless, power obtained at the output still allows an appropriate optical characterization.

Accelerometer response as a function of the gravitational field was measured using a Ferris wheel that has a controlled angular movement in such a way that the acceleration applied to the device was the projection of this magnitude to the sensible axis of the device. Results can be seen in fig. 7. As can be observed, the expected

senoidal response as a function of the angle is obtained. It has to be noted that losses shown in this figure have been re-ranged, being the zero fixed for the maximum power output. This has been done so as to determine the optical accelerometer sensitivity. It can be observed that minimum losses are not obtained at 90° and 270° , which provide with an acceleration of 0 g, but have a slight displacement to 100° and 260° . This value corresponds to a small misalignment between waveguides of $0.18 \mu\text{m}$.

Although the behaviour between the two minimum losses presents a high linearity around the point of minimum losses, it can be observed that seismic mass displacement does not cause symmetrical power variations, since at the region between 0 and 90° (and also between 270° and 360°) a tail is observed in the experimental data. This fact can be understood if it is taken into account that waveguides have passivation that has the same properties as the standard passivation in fiber optics. When the accelerometer suffers from large negative values of the acceleration, light is partially injected to the passivation, causing a decrease of the losses. This fact is not observed at positive acceleration values since the light injected in the 2nd cladding is fastly absorbed by the silicon of the seismic mass.

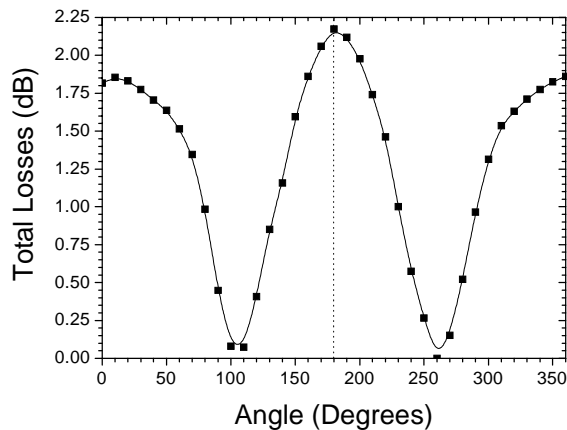


Fig. 7: Accelerometer output intensity as function of the gravity field tilt.

5.- Conclusions.

An optical accelerometer based on antiresonant waveguides has been designed so as to have an optical sensitivity of 4.6 dB/g. The fabrication process using BESOI wafers has proved its viability and reference waveguides presented the expected low radiation and insertion losses (0.3 dB/cm and 2.5 dB) at the working wavelength. Although inappropriate polishing of the V-grooves have caused a significant increase of the insertion losses, static measurements confirm the viability of using ARROW structures in MOEMS. Concertely, experimental results have proved that waveguides only are $0.18 \mu\text{m}$ misaligned, with a highly lineal but asymmetric response, due to the passivation.

6.- Acknowledgements.

The authors would like to thank **D+T MICROELECTRONICA A.I.E.** for their constant support, A. Llobera would also like to thank the

Generalitat de Catalunya (Catalan Council) for the grant 2001-TDOC-00008.

7.- Bibliography.

- [1] N.Yazdi, F.Ayazi, K.Najafi. *Micromachined Inertial Sensors*. *Proced. IEEE* 86[8], 1640-1659. 1998.
- [2] J.M.López-Higuera, P.Mottier, et al. *Optical Fiber and Integrated Optics Accelerometers for Real Time Vibration Monitoring in Harsh Environments: In-Lab and in-Field Characterization*. *Europ.Works.Opt.Fib. Sens.(SPIE)* 3483, 223-226. 1998.
- [3] J.Kalenik, R.Pajak. *A Cantilever Optical-fiber Accelerometer*. *Sens.& Act.A* 68, 350-355. 1998.
- [4] T.Baba, Y.Kokubun. *Dispersion and Radiation Loss Characteristics of Antiresonant Reflecting Optical Waveguides-Numerical Results and Analytical Expressions*. *J.Quant.Elect.* 28[7], 1689-1700. 1992.
- [5] I.Garcés, F.Villuendas, et al. *Analysis of Leakage Properties and Guiding Conditions of Rib Antiresonant Reflecting Optical Waveguides*. *J.Light.Tech.* 14[5], 798-805. 1996.